




Article

Development of a Contaminant Distribution Model for Water Supply Systems

Oluwaseye S. Adedoya ^{1,*} , Yskandar Hamam ^{1,2} , Baset Khalaf ¹ and Rotimi Sadiku ³ 

¹ French South African Institute of Technology (F'SATI)/Department of Electrical Engineering, Tshwane University of Technology, Pretoria 0001, South Africa

² École Supérieure d'Ingénieurs en Électrotechnique et Électronique, Cité Descartes, 2 Boulevard Blaise Pascal, Noisy-le-Grand, 93160 Paris, France

³ Institute of NanoEngineering Research (INER)/Department of Chemical, Metallurgy and Material Engineering, Tshwane University of Technology, Pretoria 0001, South Africa

* Correspondence: princeturn205@yahoo.com; Tel.: +27-632-482-598

Received: 21 June 2019; Accepted: 17 July 2019; Published: 21 July 2019



Abstract: Water contamination can result in serious health complications and gross socioeconomic implications. Therefore, identifying the source of contamination is of great concern to researchers and water operators, particularly, to avert the unfavorable consequences that can ensue from consuming contaminated water. As part of the effort to address this challenge, this present study proposes a novel contaminant distribution model for water supply systems. The concept of superimposing the contaminant over the hydraulic analysis was used to develop the proposed model. Four water sample networks were used to test the performance of the proposed model. The results obtained displayed the contaminant distributions across the water network at a limited computational time. Apart from being the first in this domain, the significant reduction of computational time achieved by the proposed model is a major contribution to the field.

Keywords: contaminant distribution model; hydraulic analysis; superimposing; novel scheme

1. Introduction

The provision of potable water is essential to human health and the well-being of a society. This also conforms with one of the set objectives (target 6a) of the United Nation's sustainable Development Goals (SDGs) by 2030 [1]. Despite reports that access to water have improved, a depleted delivery of potable water is an utmost concern that affects several continents. Interestingly, the goal of a utility operator is to supply water in adequate quantity and quality when desired. Usually, water is transported through water distribution networks (WDNs) from a treatment plant to consumers' taps. A WDN is a complex infrastructure, which comprises of: pipes, nodes, and reservoirs where human interference is possible. Hence, it is exposed to both accidental and intentional attacks, which can have severe consequences on the public health, besides socioeconomic implications [2,3].

Mostly, the quality of water is examined at a treatment plant, but it can technically be contaminated during transportation, through: pipe leakages, nodes and cross-connections [4]. The negative consequences of consuming contaminated water can be severe, as reported in the literature [5]. For instance, Kenzie et al. [6] and Corso et al. [7] discussed the significant impact of a transported infection through a water supply system in Milwaukee, (USA) that engendered 403,000 users, some were subsequently hospitalised with an estimated bill of about USD 96.2 million. Cooper et al. [8] reported the consequences of an accidental pollution of a chemical in a WDN in Virginia, where over 300,000 users were affected. Several studies [6–8] have also established that attacks on the WDNs are real, and can happen again. The socioeconomic implications that can arise from water network attacks

have allowed researches on water security, a notable attention and posited it at the forefront of research in this area.

Consequently, two notable preventive measures are recognised to curtail the attacks on the WDNs. These are: (1) enhancement of the physical infrastructure of the system, and (2) an instalment of water quality monitoring sensors across the water networks. An intensive monitoring of the network nodes will increase the level of safety. Unfortunately, it is impracticable to install sensors at every node in the network due to the high cost of procuring water quality monitoring sensors under limited budget constraints. In order to overcome these constraints, numerous efforts have been proposed to address the concern [9–17]. Even though an installed water quality sensor detects a contaminant event, it is imperative to identify the source of the contamination for immediate action to be taken, so as to minimise the adverse effect from contaminated water on the public health.

As such, research efforts on the Contamination Source Identification (CSI) in a water distribution network has significantly gained recognition. Modelling the transport and fate of contaminant in a WDN, demands knowledge about the characteristics of the contaminant, which are hardly known. Furthermore, it is rarely possible to identify the name of the contaminant and its type (chemical or biological); these add to the complexity encountered in developing a precise water quality model. Researchers and stakeholders have proposed various methodologies to address this challenge [13,18–23]. Adedoja et al. [5] presented a comprehensive review on how to establish a source of contamination in a water distribution network. Since hydraulic model exists and has been solved by some researchers [24–27], incorporating contaminant into it is a promising approach. Superimposing the contaminant into the hydraulic model has no effect on the flow direction. Based on this background, this study develops, a contaminant distribution model, by superimposing contaminants into the hydraulic analysis in order to quantify the contaminant distribution across the water networks. This is part of an effort to bridge the identified research shortcomings and contribute to knowledge in this domain. The rest of this paper is organised as follows: Section 2 outlines a brief background and related works. In Section 3, the description of the hydraulic model and the proposed mathematical formulation is presented. Implementation of the developed model on water networks is detailed in Section 4. Results and discussions are contained in Section 5, while conclusions and future research studies are presented in Section 6.

2. Background and Related Works

The CSI problem is characterised by responding to three (3) vital concerns: locating the source of contamination, the time of injection, and its magnitude. A derivation of the information from the data collected from water quality monitoring stations, is a complex task that must be resolved for prevention purposes, which include: public warning announcements, valves closure, pipes flushing, etc. Over the years, researchers have proposed different approaches; the use of simulation-optimisation approach [18], particle backtracking [28], machine learning [29], data mining [30], among others. CSI problem is commonly treated as an inverse problem by attempting to locate the source of contamination from the data collected from the water quality monitoring stations. Van Bloemen et al. [31] proposed a quadratic programming (QP) technique to tackle this problem. The authors' model exhibited a probable capability to address the challenge. However, excessive computational stress was identified as a shortcoming of their approach. Thereafter, Lair et al. [32] suggested a dynamic optimisation method, based on a sub-domain to curtail this computational stress. They reported that the model can merely handle the computational stress, but excludes key information during the selection of sub-domains, which was a setback of the approach.

Preis and Ostfeld [33] presented a coupled model tree-linear programming technique with the use of the commonly adopted EPANET tool developed by Rossman [34]. Preis and Ostfeld [35] proposed a combination of a Generic algorithm (GA) with the EPANET to resolve the CIS problem. EPANET was employed for the hydraulic simulation, while GA was used to moderate the injection attribute. The method minimises the difference between the measured and the evaluated data. The use of this

method requires an excessive computation that demands the use of parallel computing. In addition, the study by Liu et al. [22,23] discussed an adaptive dynamic optimisation (ADOPT) method. This method has a real-time response with contamination occurrences. The authors utilised an evolutionary algorithm (EA) to overcome the early convergence that can lead to imprecise output. This process helps to preserve a group of possible output that can lead to diverse non-unique solutions. The EA enhances the results once a new observation is absorbed, which decreases the magnitude of the non-uniqueness. It was tested by using two water networks to demonstrate the feasibility of the proposed method. The consideration of a single source of injection and non-reactive contaminants are some of the advantages of this method; however, for a large water network, such assumptions may not be feasible. The model may therefore, suffer from over-generalization. Recently, Xu et al. [19] used a cultural algorithm to address a similar concern. They demonstrated the viability of the method by using three water supply networks. The results obtained exhibited positive capability of the technique, even though extreme computation was a major setback. Other shortcomings connected to the CSI problems are: complex network nodes, and stochastic demand of water, which can lead to some problems of uncertainties. Yan et al. [36] proposed a hybrid encoding method to improve the convergence criteria.

Probabilistic and Bayesian techniques have also been used to address CSI problem. Dawsey et al. [37] proposed an inclusion of sensor data with a possibility to evaluate the source of occurrence from different areas, while Tao et al. [38] formulated a probabilistic approach. Nuepauer et al. [39] presented a backward modelling scheme with the use of a Probability Density Function (PDF) to locate the source and release time of contamination. The collected information from the monitoring sensor were used to generate the PDF. The results obtained expressed the effectiveness of the backward model to handle a steady flow conditions with a single source of the contamination. Wang and Zhou [40] applied a Bayesian sequential technique to handle the CSI problem. Baradouzi et al. [41] discussed a Probabilistic Support Vector Machines (PSVMs) technique to identify the source of contamination; they used some tools to train the PSVMs. The results obtained exhibit the feasibility of the approach to identify an upstream region viable for likely location. The water distribution system of Arak, Iran was employed to validate the proposed method.

Other notable works have been presented by Di Nardo et al. [42], model-based by Zechman and Ranjithan [20], artificial neural networks, (ANN) by Kim et al. [43] and hybrid methods [44,45] to resolve the CSI problem. Propato [13] discussed an entropic-based method. In the study, a linear algebraic technique was first employed to minimise the selection of probable sources. Thereafter, a minimum entropy method was applied to evaluate the likely source, which led to the potential sources that are sensible to the monitoring stations. An evolutionary scheme and population-based global search method was presented by Zechman and Ranjithan [20]. The technique was devised by applying a tree-based encoding model, which generates the decision vectors and a set of connected genetic operators that led to an effective search. Liu et al. [45] combined a statistical method and a heuristic search model to present the contamination incident. The statistical method pointed the possible locations and the heuristic search method amplified the contamination source attributes. The feasibility of the method was examined by using two water networks. The results obtained showed a quick adaptive discovery of contaminant attributes. However, the method cannot be expanded to handle multiple sources occurrence. Liu et al. [44] proposed a hybrid method to characterise the sources by giving a sensor measurements in real time. The method integrates a logistic regression (LR) and local improvement model to speed-up the convergence processes. In order to ascertain the capability of the method, two water networks were examined. The first is a sample small network of about 117 pipes, while the details of the second network was adapted from [46]. The results obtained, expressed the fast convergence of the hybrid method when compared to the single method. Despite the significant effort recorded on the aforementioned problem, excessive computation remained unsolved. To this end, the present study formulates a contaminant distribution model when given the source of contamination, with an assumption that hydraulic solution is solved.

3. Proposed Model Formulation

Since hydraulic model exists and have been solved by some researchers [24,26], this study proposes to superimpose the contaminant into the hydraulic analysis. This study formulates a contaminant distribution model by giving a source of contaminations and, on an assumption that the hydraulic model is resolved and the network flow analysis is known.

3.1. Hydraulic Model

By applying graph the theory, a water distribution network can be presented as a connected graph with a set of edges and a set of nodes [24]. The former consists of pipes, pumps and valves. The two basic principles that describe the hydraulic equations in a water distribution network are: the principle of mass continuity in the node and, an energy conservation around the loop. A typical water network consist of n_p number of pipes, n_j number of junction nodes (nodes with unknown heads), and n_f number of fixed-head nodes (nodes with known heads), the total number of nodes in the network can be expressed as: $n_t = n_j + n_f$. The mass continuity equation is similar to the Kirchoff's law in electrical network and, it is applicable to the nodes with known demand. It states that the algebraic summation of the flows at the node is zero. Thus, it is expressed as:

$$A_s q + d = 0 \quad (1)$$

where $q \in \mathbb{R}^{n_p \times 1} = [q_1, q_2, q_{np}]^T$ is the vector of the pipe flow rates; $d \in \mathbb{R}^{n_j \times 1} = [d_1, d_2, d_{nj}]^T$ is the vector of the fixed demand at the nodes with unknown heads and A_s is the node-pipe incidence matrix of dimension $n_j \times n_p$ connecting to the nodes with unknown heads [47]. The energy conservation law is related to the Kirchoff's voltage law in electrical network. It deals with head losses around the loops and, can be presented in term of its topological matrix as follows:

$$\bar{M} \Delta h_s = \Delta h \quad (2)$$

where Δh is the head loss vector across the pipes; Δh_s is the head loss across the loops; $\bar{M} \in \mathbb{R}^{m \times np}$ represented the loop-pipe incidence matrix; and m is the number of loops. The element \bar{M} in Equation (2) are derived from:

$$\bar{M}_{ij} = \begin{cases} +1 & \text{if pipe } j \text{ is in loop } i \text{ and is in the same direction} \\ -1 & \text{if pipe } j \text{ is in loop } i \text{ and is in the opposite direction} \\ 0 & \text{if pipe } j \text{ is not in loop } i \end{cases} \quad (3)$$

In addition, the energy conservation is expressed, thus:

$$\Delta h_s = \begin{bmatrix} A_s^T & A_f^T \end{bmatrix} \begin{bmatrix} h \\ h_f \end{bmatrix} \quad (4)$$

where $h = [h_1, h_2, \dots, h_{n_j}]^T$ denotes the vector of the unknown heads of dimension $(n_j \times 1)$ and $h_f = [h_{f(1)}, \dots, h_{f(n_f)}]^T$ represents the vector of the unknown heads of dimension $(n_f \times 1)$. A_s is the node-pipe incidence matrix of dimension $n_j \times n_p$ associating to the nodes with unknown heads [47]. Both A_s and A_f are obtained from the actual topological incidence matrix, A as:

$$A = \begin{bmatrix} A_s \\ A_f \end{bmatrix} \quad (5)$$

The element A is derived from

$$A_{ij} = \begin{cases} +1 & \text{if the flow in pipe } j \text{ leaves node } i \\ -1 & \text{if the flow in pipe } j \text{ enters node } i \\ 0 & \text{if pipe } j \text{ is not incident to node } i \end{cases} \quad (6)$$

Similarly, the head loss equations are essential for the solution of the piping networks. It describes the pressure drop across a given pipe of flow in a particular pipe. An illustration of this is described by the element shown in Figure 1, with two end nodes i and j . The head loss due to the friction of the flow of water with the pipe wall is commonly expressed as:

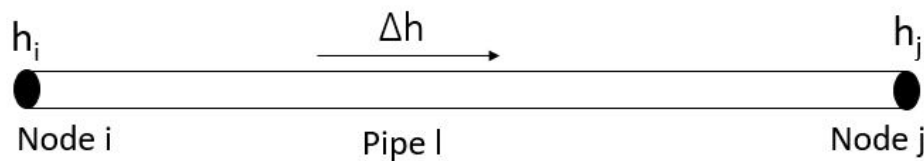


Figure 1. Network element [24].

$$\Delta h(r, q) = h_i - h_j = Eq \quad (7)$$

$$E = r|q|^{\alpha-1} \quad (8)$$

where h_i and h_j are the heads at end node of the pipe and $r = [r_1, \dots, r_{np}]^T$ denotes the vector of the pipe resistance factor. Consideration of minor loss due to the valves and other pipe connections is generally expressed in the form:

$$\Delta h(r, q) = r|q|^{\alpha-1} + k_m|q| \quad (9)$$

Subsequent, consideration of energy balance equation and the inclusion of the minor loss leads to;

$$r|q|^{\alpha-1} + k_m|q| = A_s^T h + A_f^T h_f \quad (10)$$

$$(r|q|^{\alpha-1} + k_m|q|)q - A_s^T h - A_f^T h_f = 0 \quad (11)$$

A matrix E can be defined as:

$$E = \text{diag}(r|q|^{\alpha-1} + k_m|q|) \quad (12)$$

By substituting Equations (12) into (11), the energy balance equation is expressed as

$$Eq - A_s^T h - A_f^T h_f = 0 \quad (13)$$

Equations (1) and (13) are both steady-state hydraulic equations. These can be solved in order to estimate the pipe flow and the heads at the junction node. The system of equations expressed by Equation (14) are partly linear and partly non-linear [24].

$$\begin{cases} Eq - A_s^T h - A_f^T h_f = 0 \\ A_s q + d = 0 \end{cases} \quad (14)$$

Equation (14) can also be expressed as:

$$\begin{bmatrix} E & -A_s^T \\ A_s & 0 \end{bmatrix} \begin{bmatrix} q \\ h \end{bmatrix} + \begin{bmatrix} -A_f^T h_f \\ d \end{bmatrix} = 0 \quad (15)$$

The system of equations expressed in the Equation (14) maybe solved by an iterative method. The matrix E is a $n_p \times n_p$ diagonal matrix, whose elements are formed from the head loss (including the minor loss due to valves) relation as:

$$E = \begin{bmatrix} r_1|q_1|^{\alpha-1} + k_{m1}|q_1| & \cdots & \cdots & \cdots \\ \cdots & r_2|q_2|^{\alpha-1} + k_{m2}|q_2| & \cdots & \cdots \\ \vdots & \vdots & \ddots & \vdots \\ \cdots & \cdots & \cdots & r_n|q_n|^{\alpha-1} + k_{mnp}|q_n| \end{bmatrix} \quad (16)$$

where $k_m = [k_{m1}, k_{m2}, \dots, k_{mnp}]^T$ is a $(n_p \times 1)$ vector of the minor loss factor due to valves or any other connections attached to the pipe; and α is an exponent whose value depends on the head loss model employed (1.85 for Hazen–William and 2 for both Darcy–Weisbach or Chezy–Manning head loss model) [48]. The variable r depends on the head loss model employed. In the circumstance where the Darcy–Weisbach or the Hazen–William’s model is used, the hydraulic resistance for the l^{th} pipe is described as:

$$r_l = \frac{8f_l L_l}{g\pi^2 D_l^5} \quad (17)$$

for Darcy–Weisbach model, and

$$r_l = L_l \left(\frac{3.59}{C_h w_l} \right)^{1.852} \times \frac{1}{D_l^{4.87}} \quad (18)$$

for Hazen–William model. In Equations (17) and (18), L_l is the length of the l^{th} pipe; g is the acceleration due to gravity; D_l denotes the diameter of the l^{th} pipe; f_l is a dimensionless constant, which represents the fictional factor for the l^{th} pipe; and $C_h w_l$ is the Hazen–William friction coefficient for the l^{th} pipe. The pipe friction factor f , in Equation (17) is a function of the equivalent sand roughness ε of pipes as well as the Reynold number Re , and this can be calculated by using the expression reported by Shockling et al. 2006 [49]. In this study, the Hazen–William head loss model will be adopted.

3.2. Formulation of the Proposed Contaminant Distribution Model

The formulation of this model assumes that the hydraulic solution has been resolved and the source of contaminations are known. Thus, the proposed contaminant distribution model is explicitly presented by using Figure 2.

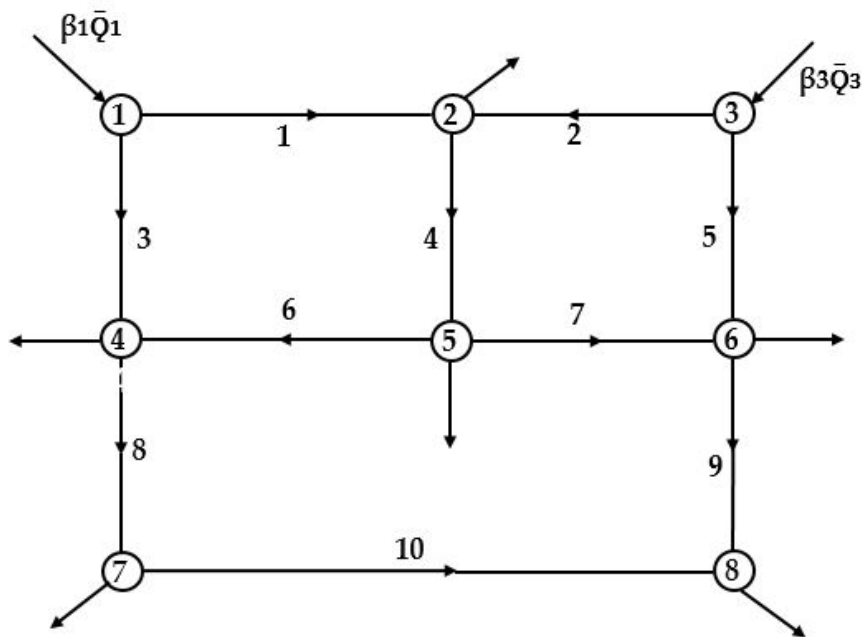


Figure 2. A sample network.

The simple network depicted in Figure 2 consists of Eight (8) nodes, and Ten (10) branches. In this case, nodes 1 and 3 are assumed to be the sources of contamination with variables; β_1 and β_3 while, the external sources are represented by; \bar{Q}_1 and \bar{Q}_3 respectively. The concentrations at nodes: 1 to 8 are independent of the inflow branches into a particular node. By assigning a variable δ_k , to the concentration at node k , the following relationships are formulated in Equations (19)–(26) as:

$$\delta_1 = \beta_1 \quad (19)$$

$$\delta_2 = \frac{\alpha_1 Q_1 + \alpha_2 Q_2}{Q_1 + Q_2} \quad (20)$$

$$\delta_3 = \beta_3 \quad (21)$$

$$\delta_4 = \frac{\alpha_3 Q_3 + \alpha_6 Q_6}{Q_3 + Q_6} \quad (22)$$

$$\delta_5 = \alpha_4 \quad (23)$$

$$\delta_6 = \frac{\alpha_7 Q_7 + \alpha_5 Q_5}{Q_5 + Q_7} \quad (24)$$

$$\delta_7 = \alpha_8 \quad (25)$$

$$\delta_8 = \frac{\alpha_9 Q_9 + \alpha_{10} Q_{10}}{Q_9 + Q_{10}} \quad (26)$$

Considering the out of the node concentrations. If concentrations in branches are represented by α_k , then Equations (26)–(33) are formulated as:

$$\alpha_1 = \alpha_3 = \delta_1 \quad (27)$$

$$\alpha_2 = \alpha_5 = \delta_3 \quad (28)$$

$$\alpha_4 = \delta_2 \quad (29)$$

$$\alpha_6 = \alpha_7 = \delta_5 \quad (30)$$

$$\alpha_8 = \delta_4 \quad (31)$$

$$\alpha_9 = \delta_6 \quad (32)$$

$$\alpha_{10} = \delta_7 \quad (33)$$

Therefore, the concentration of contamination at node k is independent of the outflow branches from the respective nodes; this is expressed in Equation (34)

$$C_{out}^t \delta_k = \alpha_k \quad (34)$$

$$C_{out} = \begin{cases} 1, & \text{if flow in branch leaves node } i \\ 0, & \text{otherwise} \end{cases} \quad (35)$$

where C_{out}^t in Equation (34) is expressed in Equation (35) and is the transpose of the incident matrices, δ_k is the concentration at node k and α_k is the concentration in branches.

Similarly, the inflow q_k , into the nodes is formulated in Equations (36)–(43) as:

$$q_1 = \bar{Q}_1 \quad (36)$$

$$q_2 = Q_1 + Q_2 \quad (37)$$

$$q_3 = \bar{Q}_3 \quad (38)$$

$$q_4 = Q_3 + Q_6 \quad (39)$$

$$q_5 = Q_4 \quad (40)$$

$$q_6 = Q_5 + Q_7 \quad (41)$$

$$q_7 = Q_8 \quad (42)$$

$$q_8 = Q_9 + Q_{10} \quad (43)$$

The matrices formulation of Equations (36)–(43) is expressed in Equation (44) as:

$$\begin{bmatrix} q_1 \\ q_2 \\ q_3 \\ q_4 \\ q_5 \\ q_6 \\ q_7 \\ q_8 \end{bmatrix} = \begin{bmatrix} 0 & 0 & 0 & 0 & 0 & 0 & 0 & 0 & 0 & 0 \\ 1 & 1 & 0 & 0 & 0 & 0 & 0 & 0 & 0 & 0 \\ 0 & 0 & 0 & 0 & 0 & 0 & 0 & 0 & 0 & 0 \\ 0 & 0 & 1 & 0 & 0 & 1 & 0 & 0 & 0 & 0 \\ 0 & 0 & 0 & 1 & 0 & 0 & 0 & 0 & 0 & 0 \\ 0 & 0 & 0 & 0 & 1 & 0 & 1 & 0 & 0 & 0 \\ 0 & 0 & 0 & 0 & 0 & 0 & 0 & 1 & 0 & 0 \\ 0 & 0 & 0 & 0 & 0 & 0 & 0 & 0 & 1 & 1 \end{bmatrix} \begin{bmatrix} Q_1 \\ Q_2 \\ Q_3 \\ Q_4 \\ Q_5 \\ Q_6 \\ Q_7 \\ Q_8 \\ Q_9 \\ Q_{10} \end{bmatrix} + \begin{bmatrix} \bar{Q}_1 \\ 0 \\ \bar{Q}_3 \\ 0 \\ 0 \\ 0 \\ 0 \\ 0 \\ 0 \\ 0 \end{bmatrix} \quad (44)$$

Equation (44) is generally expressed in Equation (45) as:

$$q_k = C_{in}^t Q_k + \bar{Q}_k \quad (45)$$

where C_{in}^t in Equation (45) is the transpose of the inflow incident matrices and expressed in Equation (46), Q_k is the flow and \bar{Q}_k , is the flow from the external sources.

$$C_{in} = \begin{cases} 1, & \text{if flow in branch leaves node } i \\ 0, & \text{otherwise} \end{cases} \quad (46)$$

The integration of the concentration at node, δ and flow at node, q can be expressed in term of flow, Q . Thus, the concentration in branches (i.e., pipes) α , are formulated and expressed in Equations (47)–(54) as:

$$\delta_1 q_1 = \beta_1 q_1 = \beta_1 \bar{Q}_1 \quad (47)$$

$$\delta_2 q_2 = \alpha_1 Q_1 + \alpha_2 Q_2 \quad (48)$$

$$\delta_3 q_3 = \beta_3 \bar{Q}_3 \quad (49)$$

$$\delta_4 q_4 = \alpha_3 Q_3 + \alpha_6 Q_6 \quad (50)$$

$$\delta_5 q_5 = \alpha_4 Q_4 \quad (51)$$

$$\delta_6 q_6 = \alpha_5 Q_5 + \alpha_7 Q_7 \quad (52)$$

$$\delta_7 q_7 = \alpha_8 Q_8 \quad (53)$$

$$\delta_8 q_8 = \alpha_9 Q_9 + \alpha_7 Q_7 \quad (54)$$

Equations (47)–(54) are represented in matrices form in Equation (55)

$$\begin{bmatrix} \delta_1 q_1 \\ \delta_2 q_2 \\ \delta_3 q_3 \\ \delta_4 q_4 \\ \delta_5 q_5 \\ \delta_6 q_6 \\ \delta_7 q_7 \\ \delta_8 q_8 \end{bmatrix} = \begin{bmatrix} 0 & 0 & 0 & 0 & 0 & 0 & 0 & 0 & 0 & 0 \\ 1 & 1 & 0 & 0 & 0 & 0 & 0 & 0 & 0 & 0 \\ 0 & 0 & 0 & 0 & 0 & 0 & 0 & 0 & 0 & 0 \\ 0 & 0 & 1 & 0 & 0 & 1 & 0 & 0 & 0 & 0 \\ 0 & 0 & 0 & 1 & 0 & 0 & 0 & 0 & 0 & 0 \\ 0 & 0 & 0 & 0 & 1 & 0 & 1 & 0 & 0 & 0 \\ 0 & 0 & 0 & 0 & 0 & 0 & 0 & 1 & 0 & 0 \\ 0 & 0 & 0 & 0 & 0 & 0 & 0 & 0 & 1 & 1 \end{bmatrix} \begin{bmatrix} \alpha_1 Q_1 \\ \alpha_2 Q_2 \\ \alpha_3 Q_3 \\ \alpha_4 Q_4 \\ \alpha_5 Q_5 \\ \alpha_6 Q_6 \\ \alpha_7 Q_7 \\ \alpha_8 Q_8 \\ \alpha_9 Q_9 \\ \alpha_{10} Q_{10} \end{bmatrix} + \begin{bmatrix} \beta_1 \bar{Q}_1 \\ 0 \\ \beta_3 \bar{Q}_3 \\ 0 \\ 0 \\ 0 \\ 0 \\ 0 \\ 0 \\ 0 \end{bmatrix} \quad (55)$$

The general formulation of Equation (55) is expressed in Equation (56) as:

$$\left[\text{diag}(q) \delta = C_{in}^t \text{diag}(Q) \alpha + \text{diag}(\bar{Q}) \beta \right] \quad (56)$$

The concentration in branches α , is related to the concentration at node δ and is expressed in Equation (57) as:

$$\begin{bmatrix} \alpha_1 \\ \alpha_2 \\ \alpha_3 \\ \alpha_4 \\ \alpha_5 \\ \alpha_6 \\ \alpha_7 \\ \alpha_8 \\ \alpha_9 \\ \alpha_{10} \end{bmatrix} = \begin{bmatrix} 1 & 0 & 0 & 0 & 0 & 0 & 0 & 0 & 0 \\ 0 & 0 & 1 & 0 & 0 & 0 & 0 & 0 & 0 \\ 1 & 0 & 0 & 0 & 0 & 0 & 0 & 0 & 0 \\ 0 & 1 & 0 & 0 & 0 & 0 & 0 & 0 & 0 \\ 0 & 0 & 1 & 0 & 0 & 0 & 0 & 0 & 0 \\ 0 & 0 & 0 & 0 & 1 & 0 & 0 & 0 & 0 \\ 0 & 0 & 0 & 0 & 1 & 0 & 0 & 0 & 0 \\ 0 & 0 & 0 & 1 & 0 & 0 & 0 & 0 & 0 \\ 0 & 0 & 0 & 0 & 0 & 1 & 0 & 0 & 0 \\ 0 & 0 & 0 & 0 & 0 & 0 & 1 & 0 & 0 \end{bmatrix} \begin{bmatrix} \delta_1 \\ \delta_2 \\ \delta_3 \\ \delta_4 \\ \delta_5 \\ \delta_6 \\ \delta_7 \\ \delta_8 \end{bmatrix} \quad (57)$$

Equation (57) is generally expressed in Equation (58) as:

$$\left[\alpha = C_{out} \delta \right] \quad (58)$$

If Equation (58) is substituted into Equation (56), then, Equation (59) is expressed as:

$$\text{diag}(q)\delta = \left[C_{in}^t \text{diag}(Q) C_{out} \right] \delta + \text{diag} \bar{Q} \beta \quad (59)$$

$$\left[\text{diag}(q) - C_{in}^t \text{diag}(Q) C_{out} \right] \delta = \text{diag} \bar{Q} \beta \quad (60)$$

By resolving Equation (60), δ may be derived. Therefore, the distribution of contaminants across the pipes and at the nodes can be quantified.

4. Application of the Developed Model on WDNs

The validation of the developed contaminant distribution model was implemented on four water distribution networks, which were adapted from literature [47,50,51]. All computations and hydraulic analysis were performed in MATLAB software environment.

4.1. Model Programming Procedures

This procedure assumes that the hydraulic network analysis has been resolved. In this study, Newton–Raphson’s Content Model solution is employed [24]. The required input from the solved network analysis are; sending nodes, receiving nodes and the flow L/s . Thus, the program procedures are as follow:

1. Get the network analysis solution
2. Prepare the Structure
3. Get the pipe flows
4. Get supplies and demands
5. Get injections at the supply nodes
6. Get contamination at supply nodes
7. Compute the sum input flows to the nodes
8. Build matrices for equation as function of gamma, δ .
9. Compute contamination at the nodes
10. Get contamination in the pipes, α .

4.2. Illustrative Example 1

Figure 3 is a water distribution network adapted from the work of Ozger [50], to demonstrate the validity of the developed contaminant distribution model. The network has two (2) reservoirs with twenty-one (21) Pipes, and (13) thirteen Nodes. In this example, it is assumed that 3% and 2% of the flow are injected at reservoir 1 and 2 as contaminants, respectively. The available network characteristics are presented in Table 1.

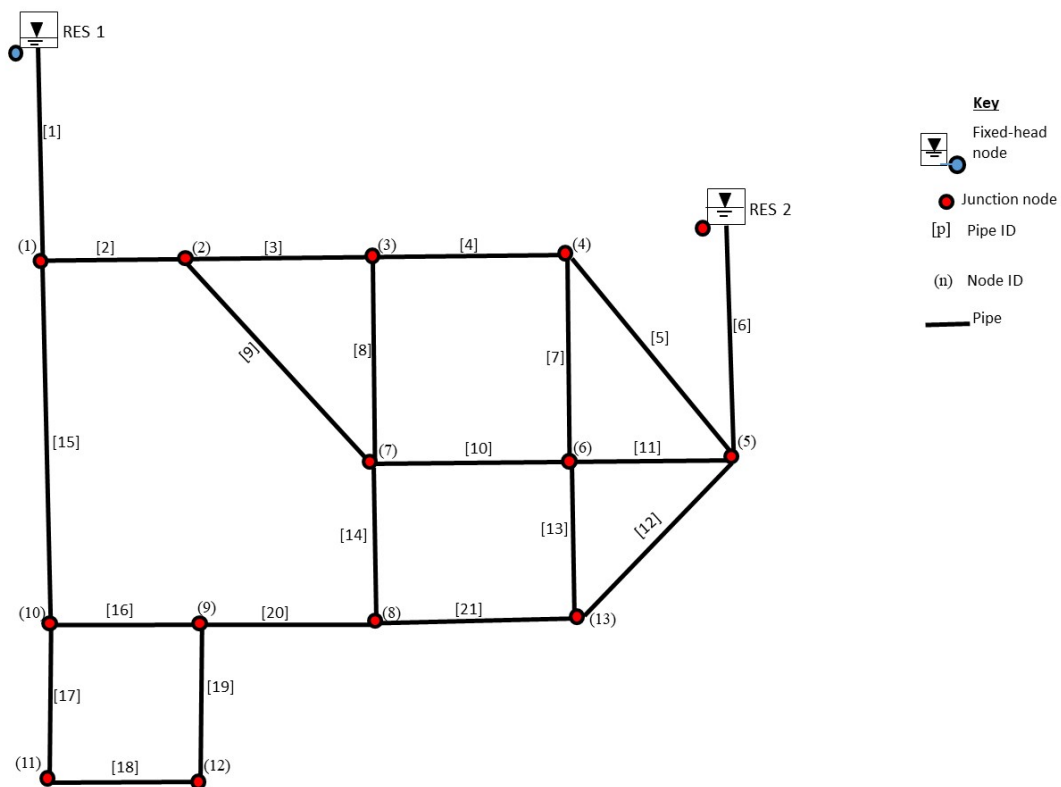


Figure 3. Schematic for Illustrative Example 1 Ozger [50].

Table 1. Pipe characteristics.

Pipe ID	Length (m)	D (mm)	C (H-W)	Node ID	Elevation (m)	Demand (CMH)
1	609.60	762	130	1	27.43	0.0
2	243.80	762	128	2	33.53	212.4
3	1524.00	609	126	3	28.96	212.4
4	1127.76	609	124	4	32.00	640.8
5	1188.72	406	122	5	30.48	212.4
6	640	406	120	6	31.39	684.0
7	762.00	254	118	7	29.56	640.8
8	944.88	254	116	8	31.39	327.6
9	1676.40	381	114	9	32.61	0.0
10	883.92	305	112	10	34.14	0.0
11	883.92	305	110	11	35.05	108.0
12	1371.60	381	108	12	36.58	108.0
13	762.00	254	106	13	33.53	0.0
14	822.96	254	104	RES	60.96	N/A
15	944.88	305	102	RES	60.96	N/A
16	579.00	305	100			
17	487.68	203	98			
18	457.20	152	96			
19	502.92	203	94			
20	883.92	203	92			
21	944.88	305	90			

4.3. Illustrative Example 2

This example consists of 71 pipes, 46 nodes and a reservoir. The details of the Illustrative Example 2 for the validation of the developed model was adapted from Kumar et al. [51]. The schematic of Illustrative Example 2 is shown in Figure 4.

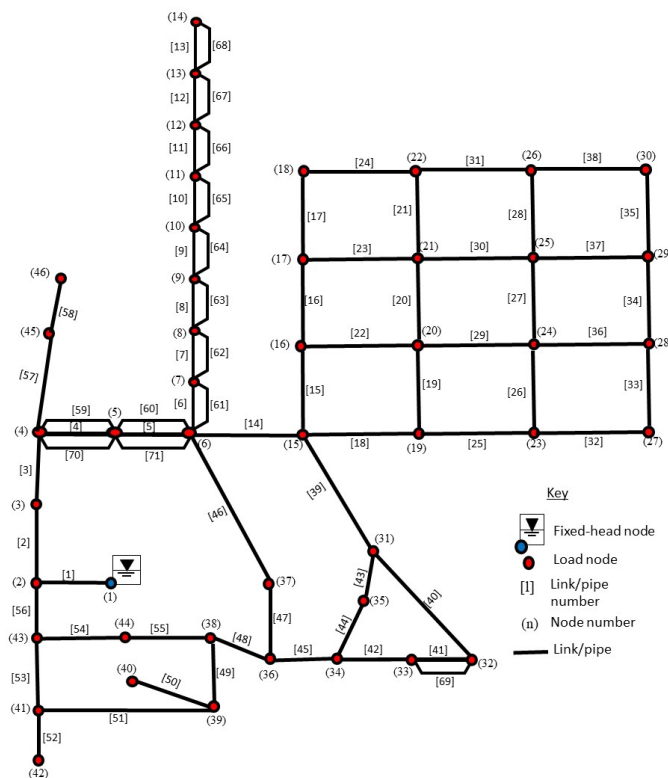


Figure 4. Schematic for Illustrative Example 2 Kumar et al. [51].

4.4. Illustrative Example 3

In this example, one hundred and five (105) pipes network depicted in Figure 4, was considered. The network consists of 105 pipes, three fixed-head nodes (sources), and 64 nodes, after redundant nodes (these are nodes where two or more pipes meet with zero demand) were removed. The network characteristic data defining the network is available in the report of Adedeji [47].

4.5. Illustrative Example 4

This example examined the four hundred and forty two pipes as represented in Figure 5. The network contains 442 pipes, three reservoirs, and 295 nodes after the redundant (these are nodes where two or more pipes meet with zero demand) nodes have been removed. The data defining the network is available in the report by Adedeji [47].

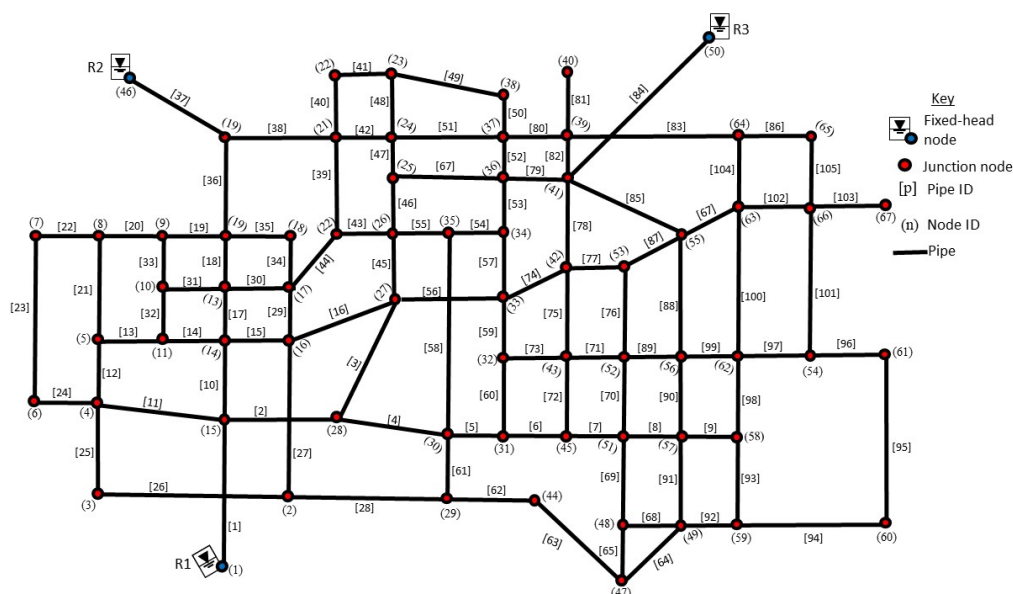


Figure 5. Schematic for Illustrative Example 3 Adedeji [47].

5. Results and Discussions

This section presents the results and discussions of the four (4) sample networks examined for the validation of the performance of the developed model. Tables 2 and 3 present the numerical results for illustrative Example 1.

5.1. Results and Discussions for Illustrative Example 1

The results of the pipe flow and the contaminant in the pipes are presented in Table 2. This Table shows that Pipe 7 has contaminant concentration of 0.029; it is as a result of the combination of the contaminants from Nodes 1 and 2 at Node 4. At Pipes 5, 6, 11, 12, and 21, the contaminants are from the same source, Node 2, while the other pipes have the same contaminant concentration (0.030); this implies that the contaminant is from Node 1. Based on these results, pipes with the same node as origin, have the same contaminant concentration, for example, Pipes, 5, 6, 11, 12, and 21. However, where different contaminant mix at a node, the contaminant concentration that will leave the node will be less than the maximum contaminant concentration that enters the node. A typical example of this scenario is at Pipe 7. On the other hand, when the quantity of contaminants from different pipes meeting at a node are the same, the contaminant concentration leaving the node will be the average of the contaminant concentration that entered into the node. Thus, this shows that the proposed model results are realistic.

Table 2. Numerical results for pipe and contaminant flow for illustrative Example 1.

Pipe ID	Pipes Flow Rate (L/s)	Contaminant in Pipes (L/s)	% of Contaminant in Pipes
1	625.874	18.776	0.030
2	625.874	18.776	0.030
3	336.585	10.098	0.030
4	219.708	6.591	0.030
5	18.485	0.369	0.020
6	248.126	4.963	0.020
7	60.193	1.758	0.029
8	57.877	1.736	0.030

Table 2. Cont.

Pipe ID	Pipes Flow Rate (L/s)	Contaminant in Pipes (L/s)	% of Contaminant in Pipes
9	151.430	4.542	0.030
10	10.287	0.308	0.030
11	84.557	1.691	0.020
12	86.082	1.721	0.020
13	34.961	0.699	0.020
14	21.021	0.631	0.030
15	78.858	2.365	0.030
16	45.785	1.373	0.030
17	33.072	0.992	0.030
18	3.0726	0.0921	0.030
19	26.927	0.807	0.030
20	18.858	0.565	0.030
21	51.120	1.022	0.020

The nodal flow and contaminant distribution at nodes for illustrative Example 1, is shown in Table 3. The results in this Table shows that Nodes 4 (0.029), 6 (0.024), and 8 (0.024) have different contaminant concentrations. These concentrations are different from the injected contaminant concentrations, which are 0.030 and 0.020 from Nodes 1 and 2, respectively. This difference in the contaminants' concentration is due to different contaminants mixing at a node. On the other hand, when different sources with the contaminant concentrations mix at a node, the node's contaminant concentration is the same as its source concentration.

Table 3. Numerical results for illustrative Example 1 for the nodes.

Node ID	Node Flow Rate (L/s)	Contaminant in Nodes (L/s)	% of Contaminant at Nodes
1	625.874	18.776	0.030
2	625.874	18.776	0.030
3	336.585	10.098	0.030
4	238.193	6.955	0.029
5	248.125	4.962	0.020
6	190.000	4.465	0.024
7	209.307	6.279	0.030
8	91.000	2.220	0.024
9	45.785	1.373	0.030
10	78.858	2.365	0.030
11	33.072	0.992	0.030
12	30	0.900	0.030
13	86.082	1.721	0.020
14	625.874	18.776	0.030
15	248.125	4.962	0.0200

5.2. Results and Discussions for Illustrative Example 2

Tables 4 and 5 present the numerical results of contaminant contribution for the pipes and nodes for illustrative Example 2. The Illustrative Example 2, as shown in Figure 4, has only one source of supply, and 5% of the flow is assumed as contaminant. Since, there is no contaminant mix, it is reasonable for the 0.050 contaminants injected at the source to flow through the entire network, which also verified the feasibility of the proposed model. The results of the pipes and nodes flow rate are also presented. A sub-network with area nodes: 15, 18, 30 and 27 revealed that the quantity of contaminants decreases from node 15 towards node 18. Similar attribute was observed from node 15 towards node 27. Perhaps, if there is a need for water piping extension, it will be appropriate to tap

from the extreme nodes, irrespective of the node position. This is because, nodes at the extreme nodes have lower quantity of contaminants. It was generally observed that the farther the node from the source of supply, the lower the quantity of contaminant at the nodes junction.

Table 4. Numerical results for pipe and contaminant flow for Illustrative Example 2.

Pipe ID	Pipes Flow Rate (L/s)	Contaminant in Pipes (L/s)	Pipe ID	Pipes Flow Rate (L/s)	Contaminant in Pipes (L/s)
1	88.879	4.444	37	0.277	0.014
2	61.733	3.086	38	0.034	0.017
3	58.003	2.900	39	6.542	0.327
4	24.731	1.236	40	1.493	0.075
5	22.966	1.148	41	0.117	0.006
6	7.490	0.374	42	2.167	0.108
7	6.545	0.327	43	0.498	0.025
8	5.880	0.294	44	0.831	0.042
9	4.805	0.240	45	3.818	0.191
10	3.415	0.171	46	2.335	0.117
11	2.530	0.126	47	1.452	0.073
12	1.865	0.093	48	3.376	0.169
13	0.733	0.037	49	1.790	0.089
14	22.758	1.137	50	0.632	0.032
15	5.362	0.268	51	0.482	0.241
16	2.266	0.113	52	2.080	0.104
17	0.776	0.038	53	14.962	0.748
18	8.014	0.401	54	5.924	0.296
19	2.479	0.124	55	5.734	0.286
20	1.6445	0.082	56	25.816	1.290
21	0.685	0.034	57	9.850	0.493
22	1.8360	0.092	58	3.660	0.183
23	0.479	0.024	59	7.967	0.398
24	0.043	0.002	60	7.398	0.369
25	5.029	0.252	61	7.490	0.374
26	1.313	0.065	62	6.545	0.327
27	0.942	0.471	63	5.880	0.294
28	0.401	0.020	64	4.805	0.240
29	1.913	0.095	65	3.415	0.171
30	0.809	0.040	66	2.530	0.126
31	0.264	0.013	67	1.865	0.093
32	2.832	0.141	68	1.797	0.089
33	0.137	0.007	69	0.117	0.006
34	0.509	0.025	70	11.606	0.580
35	0.345	0.017	71	10.778	0.538
36	1.025	0.051			

Table 5. Numerical results for node and contaminant flow for Illustrative Example 2.

Node ID	Node Flow Rate (L/s)	Contaminant in Nodes (L/s)	Node ID	Nodes Flow Rate (L/s)	Contaminant in Nodes (L/s)
1	88.879	4.444	24	3.227	0.161
2	88.879	4.444	25	1.749	0.087
3	61.732	3.086	26	0.665	0.033
4	58.003	2.900	27	2.970	0.148
5	44.303	2.215	28	1.024	0.051
6	41.143	2.057	29	0.786	0.039
7	14.980	0.749	30	0.378	0.018
8	13.090	0.654	31	6.542	0.327
9	11.760	0.588	32	1.493	0.074
10	9.610	0.481	33	2.400	0.120
11	6.830	0.342	34	3.818	0.191
12	5.060	0.253	35	1.330	0.066
13	3.730	0.186	36	4.828	0.241
14	2.530	0.126	37	2.335	0.116
15	22.757	1.137	38	5.734	0.287
16	5.362	0.268	39	2.272	0.113
17	2.266	0.113	40	0.632	0.032
18	0.820	0.041	41	14.962	0.748
19	8.014	0.401	42	2.080	0.104
20	4.315	0.215	43	25.816	1.290
21	2.123	0.106	44	5.924	0.296
22	0.685	0.034	45	9.850	0.492
23	5.029	0.251	46	3.660	0.183

5.3. Results and Discussions for Illustrative Example 3

Tables 6 and 7 present the numerical results of the contaminant contribution across the pipes and the nodes for illustrative Example 3. In this example, it was assumed that Nodes 1, 46, and 50 are sources of contamination with 0.04, 0.05 and 0.03 contaminants, respectively. This example has redundant nodes (these are nodes where two or more pipes meet with zero demand), which were excluded in the simulations. The node numerical results obtained (Table 7) revealed that most of the nodes have different contaminant values from injected contaminants at the three (3) sources (Nodes; 1, 46, and 50) of contamination. This is due to the fact that, different contaminants mix at different nodes of the networks. It was observed that the contaminant (0.04) at source (Node 1) flows through Node 1 to 6; 10–11; 14–16; 27 and 28, respectively. These nodes have direct connections to the source (Node 1) without mixing with the two sources of contaminant, as can be seen in the schematic diagram of the network in Figure 5. Similarly, the contaminant from source (Node 46) flows through Nodes; 46, 19, 21, and 22, respectively. These nodes are also directly connected to the source (Node 46) without any interconnected nodes from other sources of contamination. This same attribute was observed from source (Node 50) where Nodes; 41, 36, 34, 35, 33, 41, 53 and 55 have the same contaminant values that was injected at source (Node 50). On the other hand, contaminant at the remaining nodes differ from the injected values (ranges between the lowest to highest values. i.e., 0.030–0.050). Based on the results obtained, the values of contaminants from Nodes 7–13 range between the contaminant values from Nodes 1 and 46 (i.e., 0.040–0.050). The results showed that these nodes have contaminant mixtures from the stated nodes (i.e., Nodes 1 and 46). Similar attribute was observed at Nodes; 17, 18, 20, 23, and 24. The results of the remaining nodes indicated a mixture of contaminants from source Nodes 1 and 50. These can be seen from the numerical results for Nodes 47 to 67. Moreover, circumstances where three contaminants mix at the nodes are possible within the network. This further established the practicability of the proposed model as observed from the results.

Table 6. Numerical results for pipe and contaminant flow for Illustrative Example 3.

Pipe ID	Pipes Flow Rate (L/s)	Contaminant in Pipes (L/s)	% in Pipes	Pipe ID	Pipes Flow Rate (L/s)	Contaminant in Pipes (L/s)	% in Pipes
1	333.826	13.353	0.0400	54	3.202	0.096	0.0300
2	203.906	8.156	0.0400	55	0.872	0.026	0.0300
3	80.237	3.209	0.0400	56	13.062	0.522	0.0400
4	123.668	4.946	0.0400	57	2.922	0.087	0.0300
5	77.794	3.097	0.0398	58	2.329	0.069	0.0300
6	74.988	2.985	0.0398	59	7.701	0.275	0.0358
7	71.229	2.836	0.0398	60	2.805	0.112	0.0398
8	27.487	1.094	0.0398	61	8.204	0.326	0.0398
9	13.357	0.527	0.0395	62	12.085	0.481	0.0399
10	68.823	2.752	0.0400	63	2.914	0.115	0.0397
11	51.096	2.043	0.0400	64	8.716	0.347	0.0397
12	21.911	0.876	0.0400	65	4.198	0.166	0.0396
13	14.557	0.582	0.0400	66	3.970	0.158	0.0398
14	23.466	0.938	0.0400	67	12.686	0.505	0.0398
15	7.850	0.314	0.0400	68	26.055	1.037	0.0398
16	21.783	0.871	0.0400	69	12.558	0.437	0.0348
17	37.507	1.500	0.0400	70	3.759	0.149	0.0398
18	11.772	0.473	0.0420	71	10.506	0.387	0.0368
19	4.206	0.192	0.0458	72	6.717	0.201	0.0300
20	3.183	0.145	0.0458	73	8.292	0.248	0.0300
21	16.468	0.658	0.0400	74	0.003	0.001	0.0300
22	9.651	0.395	0.0409	75	40.705	1.221	0.0300
23	0.348	0.014	0.0400	76	55.714	1.671	0.0300
24	10.348	0.414	0.0400	77	42.031	1.261	0.0300
25	3.837	0.153	0.0400	78	26.066	1.007	0.0387
26	1.1627	0.046	0.0400	79	10.000	0.352	0.0353
27	10.043	0.401	0.0400	80	16.945	0.508	0.0300
28	3.881	0.155	0.0400	81	23.012	0.811	0.0353
29	19.590	0.783	0.0400	82	125.101	3.753	0.0300
30	4.332	0.181	0.0419	83	10.408	0.312	0.0300
31	10.067	0.404	0.0402	84	40.708	1.221	0.0300
32	8.909	0.356	0.0458	85	4.481	0.134	0.0300
33	1.023	0.046	0.0458	86	23.611	0.901	0.0382
34	6.834	0.286	0.0419	87	3.467	0.127	0.0369
35	8.165	0.373	0.0458	88	12.597	0.497	0.0395
36	15.599	0.780	0.0500	89	7.369	0.291	0.0396
37	76.072	3.803	0.0500	90	0.354	0.014	0.0395
38	60.472	3.023	0.0500	91	7.723	0.305	0.0396
39	6.170	0.308	0.0500	92	2.724	0.107	0.0396
40	10.570	0.528	0.0500	93	7.276	0.271	0.0373
41	5.570	0.278	0.0500	94	8.547	0.319	0.0373
42	43.732	2.186	0.0500	95	3.003	0.118	0.0395
43	5.407	0.214	0.3970	96	14.625	0.539	0.0369
44	11.577	0.523	0.0452	97	4.080	0.152	0.0373
45	25.390	1.015	0.0400	98	1.271	0.047	0.0373
46	20.857	0.827	0.3970	99	28.454	0.874	0.0307
47	14.500	0.500	0.3450	100	30.000	0.931	0.0310
48	35.090	1.619	0.0461	101	12.261	0.376	0.0307
49	20.660	0.964	0.0467	102	0.273	0.009	0.0337
50	5.660	0.264	0.0467	103	36.635	1.099	0.0300
51	8.142	0.375	0.0461	104	5.273	0.177	0.0337
52	12.263	0.367	0.0300	105	23.644	0.709	0.0300
53	6.124	0.183	0.0300				

Table 7. Numerical results of node and contaminant flow for Illustrative Example 3.

Node ID	Nodes Flow Rate (L/s)	Contaminant in Nodes (L/s)	% in Nodes	Node ID	Nodes Flow Rate (L/s)	Contaminant in Nodes (L/s)	% in Nodes
1	333.826	13.353	0.0400	35	3.202	0.096	0.0300
2	10.043	0.402	0.0400	36	42.013	1.261	0.0300
3	5.000	0.200	0.0400	37	26.066	1.008	0.0387
4	51.096	2.044	0.0400	38	20.660	0.964	0.0467
5	36.486	1.458	0.0400	39	43.012	1.516	0.0353
6	10.348	0.414	0.0400	40	10.000	0.353	0.0353
7	10.000	0.409	0.0409	41	125.101	3.753	0.0300
8	19.651	0.804	0.0409	42	55.714	1.671	0.0300
9	4.206	0.193	0.0458	43	22.558	0.785	0.0348
10	19.999	0.808	0.0404	44	15.000	0.597	0.0398
11	23.466	0.939	0.0400	45	74.072	2.985	0.0398
12	27.371	1.253	0.0458	46	76.072	3.804	0.0500
13	41.840	1.682	0.0402	47	12.914	0.513	0.0397
14	68.823	2.753	0.0400	48	12.686	0.505	0.0398
15	333.826	13.353	0.0400	49	16.567	0.655	0.0396
16	29.633	1.185	0.0400	50	125.101	3.753	0.0300
17	31.167	1.306	0.0419	51	71.229	2.836	0.0398
18	15.000	0.660	0.0440	52	38.617	1.475	0.0382
19	76.070	3.804	0.0500	53	40.705	1.221	0.0300
20	11.577	0.523	0.0452	54	8.547	0.319	0.0373
21	60.472	3.024	0.0500	55	51.117	1.534	0.0300
22	10.570	0.529	0.0500	56	28.092	1.036	0.0369
23	40.660	1.897	0.0467	57	30.954	1.222	0.0395
24	58.232	2.687	0.0461	58	13.352	0.527	0.0395
25	44.500	1.536	0.0345	59	7.723	0.305	0.0396
26	26.263	1.042	0.0397	60	7.723	0.305	0.0396
27	80.237	3.209	0.0400	61	10.000	0.379	0.0379
28	203.906	8.156	0.0400	62	17.628	0.658	0.0373
29	12.085	0.482	0.0399	63	40.716	1.251	0.0307
30	125.998	5.016	0.0398	64	35.273	1.188	0.0337
31	77.793	3.097	0.0398	65	5.273	0.177	0.0337
32	10.506	0.387	0.0358	66	30.000	0.931	0.0310
33	22.701	0.811	0.0300	67	30.000	0.931	0.0310
34	6.124	0.184	0.0300				

The numerical results of pipe and contaminant flow for the Illustrative Example 3 is presented in Table 6. Similar to the node results, it was observed that pipes that are directly connected to the sources of contaminants have same flow as their sources. For instances, Pipes 1–4, 10–17, 23–29 are directly connected to source (Node 1). Similar scenarios are observed in Pipes; 36–42, which are connected to source (Node 46). Likewise, the Pipes connected to source (Node 50) are 52–55, 57–58, 72–77, 80, 82–85, and 105, respectively. The rest of the pipes are connected to the nodes where two or more contaminants mix as noted from the results obtained.

5.4. Results and Discussions for Illustrative Example 4

After the removal of redundant nodes (these are nodes where two or more pipes meet with zero demand), the illustrative Example 4 network consists, 442 pipes, three reservoirs, and 295 nodes as depicted in Figure 6. This network sample is bigger than Example 3 network, and they both have three sources of contaminations. In this case, nodes 1, 116, and 164 are assumed to be contamination sources with; 0.02, 0.01, and 0.03, respectively. The contaminant distributions across this network displayed

the same attributes as the results of the Illustrative Example 3. The proposed method shows capability to handle medium networks within a short time. The results of Illustrative Example 4 is not presented due to its volume.

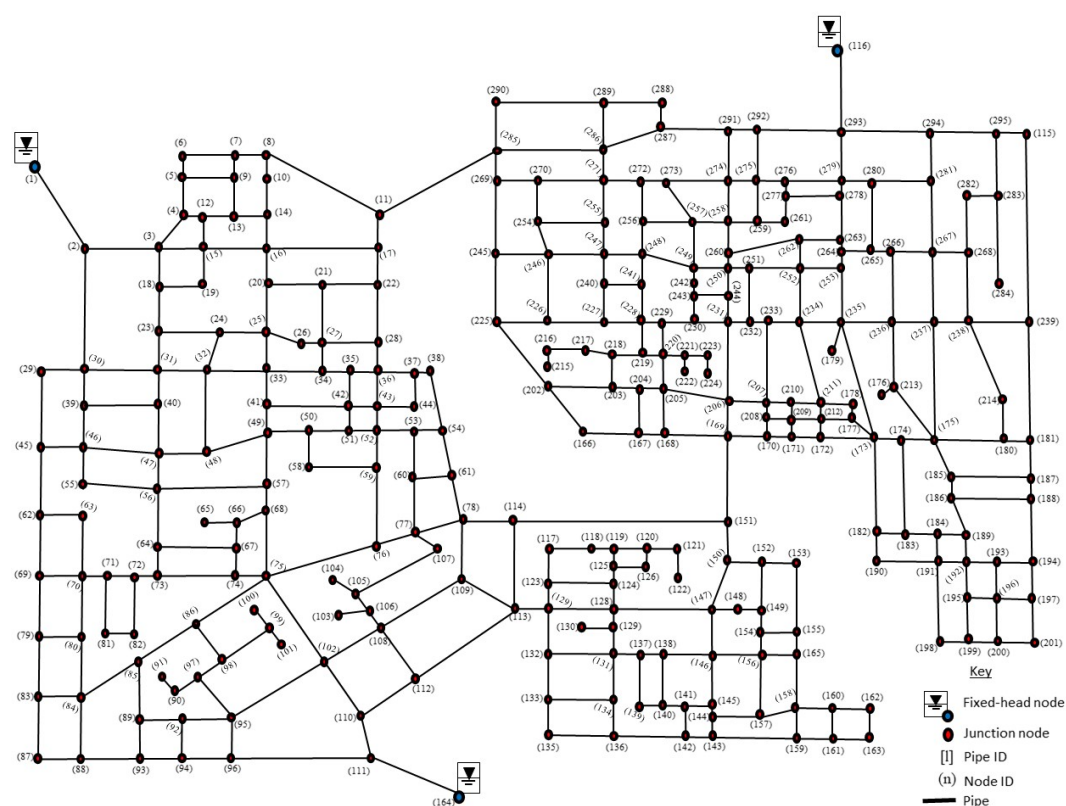


Figure 6. Schematic for Illustrative Example 3 Adedeji [47].

Table 8 shows the number of iterations taken in order to obtain the result for the various WDNs considered. As expected, the number of iterations increases as the size of the WDN increases.

Table 8. Comparison of Case Study and Iterative Period.

Case Study	Pipe Size	Node Size	No of Iteration for Network Analysis (Max = 20)
Ozger 2003 [50]	21	15	4
Kumar 2008 [51]	71	46	5
Adedeji 2018 [47]	105	67	6
Adedeji 2018 [47]	442	295	12

Table 9 depicts the execution time for both hydraulic analysis and the proposed model for the various WDNs considered in this study. It was generally observed that the bigger the network, the higher the execution time.

Table 9. Comparison of Computational time for Hydraulic Analysis and Proposed Model.

Case Study	Pipe Size	Node Size	Network Analysis Ex. Time (ms)	Proposed Model Ex. Time (ms)
Ozger 2003 [50]	21	15	35	11
Kumar 2008 [51]	71	46	41	16
Adedeji 2018 [47]	105	67	56	25
Adedeji 2018 [47]	442	295	92	44

6. Conclusions and Future Studies

Over the years, identification of contamination sources has received a significant attention among researchers and, has been a concern due to the negative effect that can emanate from the use of contaminated water. As part of an effort to fill this research gap, this study proposed a contaminant distribution model by superimposing the contaminant over the network analysis. To the best of the authors' knowledge, there is no record of this approach in the literature. The viability of the proposed model was tested with four water networks, and the model's performance was satisfactory. The results obtained described the practicability of the contaminant distribution across pipes and the nodes of the water networks. In addition, the results verified the practicability of the proposed model at a limited computational time. The source of contamination could be derived with this distribution model if, a set of measurement data is given. Thus, this will allow water supply companies to know the source of contamination upon which appropriate preventive measures such as; public awareness, closure of valves, etc. would be provided in order to minimise the extent of contamination on the society. In addition, comparison of this model with similar methodologies is important in order to ascertain its strength and weakness which, would be examined in future studies. Furthermore, procurement and maintenance cost of water quality monitoring sensor is also a challenge that must be addressed. Future research would focus on the issue of contamination source identification and optimal sensor placement in a water distribution network. The proposed model and its solution will be embedded within a method that allows the detection of the source of contamination. Although, this model was applied on a small and medium WDNs due to data availability, application of the proposed model on large networks would also be investigated in the future. These are topical areas of research interest that would be examined in subsequent studies. Finally, in order to increase the dynamics and robustness of the proposed model, it is expected that future research will explore the effects of external factors, such as temperature, on the contaminant distribution model.

Author Contributions: The work is part of the Doctorate degree of O.S.A. which was discussed with his supervisors. O.S.A. formulated the problem and drafted the manuscript. Y.H. assisted with quality improvement in the mathematical formulations and programming. The manuscript was scrutinized by Y.H. and R.S. while, B.K. also gave some suggestions.

Acknowledgments: This research work was supported by the French South African Institute of Technology (F'SATI), Tshwane University of Technology, Pretoria, South Africa.

Conflicts of Interest: The authors declare no conflict of interest.

References

1. Sdgreport. The Sustainable Development Goals 2015. 2015. Available online: www.undp.org/content/undp/en/home/sustainable-development-goals/goal-6-clean-water-and-sanitation.html (accessed on 18 May 2019).
2. Clark, R.M.; Grayman, W.M.; Males, R.M. Contaminant propagation in distribution systems. *J. Environ. Eng.* **1988**, *114*, 929–943. [[CrossRef](#)]
3. Clark, R.M.; Deininger, R.A. Protecting the nation's critical infrastructure: The vulnerability of US water supply systems. *J. Contingencies Crisis Manag.* **2000**, *8*, 73–80. [[CrossRef](#)]
4. Kirmeyer, G.J.; Martel, K. *Pathogen Intrusion into the Distribution System*; American Water Works Association: Denver, CO, USA, 2001.
5. Adedola, O.S.; Hamam, Y.; Khalaf, B.; Sadiku, R. Towards Development of an Optimization Model to Identify Contamination Source in a Water Distribution Network. *Water* **2018**, *10*, 579. [[CrossRef](#)]
6. Mac Kenzie, W.R.; Hoxie, N.J.; Proctor, M.E.; Gradus, M.S.; Blair, K.A.; Peterson, D.E.; Kazmierczak, J.J.; Addiss, D.G.; Fox, K.R.; Rose, J.B.; et al. A massive outbreak in Milwaukee of Cryptosporidium infection transmitted through the public water supply. *N. Engl. J. Med.* **1994**, *331*, 161–167. [[CrossRef](#)] [[PubMed](#)]
7. Corso, P.S.; Kramer, M.H.; Blair, K.A.; Addiss, D.G.; Davis, J.P.; Haddix, A.C. Costs of illness in the 1993 waterborne Cryptosporidium outbreak, Milwaukee, Wisconsin. *Emerg. Infect. Dis.* **2003**, *9*, 426. [[CrossRef](#)] [[PubMed](#)]

8. Cooper, W.J. Responding to crisis: The West Virginia chemical spill. *Environ. Sci. Technol.* **2014**, *48*, 3095. [[CrossRef](#)] [[PubMed](#)]
9. Berry, J.W.; Fleischer, L.; Hart, W.E.; Phillips, C.A.; Watson, J.P. Sensor placement in municipal water networks. *J. Water Resour. Plan. Manag.* **2005**, *131*, 237–243. [[CrossRef](#)]
10. Berry, J.; Carr, R.D.; Hart, W.E.; Leung, V.J.; Phillips, C.A.; Watson, J.P. Designing contamination warning systems for municipal water networks using imperfect sensors. *J. Water Resour. Plan. Manag.* **2009**, *135*, 253–263. [[CrossRef](#)]
11. Ostfeld, A.; Salomons, E. Optimal layout of early warning detection stations for water distribution systems security. *J. Water Resour. Plan. Manag.* **2004**, *130*, 377–385. [[CrossRef](#)]
12. Ostfeld, A.; Salomons, E. Optimal early warning monitoring system layout for water networks security: Inclusion of sensors sensitivities and response delays. *Civ. Eng. Environ. Syst.* **2005**, *22*, 151–169. [[CrossRef](#)]
13. Propato, M. Contamination warning in water networks: General mixed-integer linear models for sensor location design. *J. Water Resour. Plan. Manag.* **2006**, *132*, 225–233. [[CrossRef](#)]
14. Kansal, M.; Dorji, T.; Chandniha, S.K. Design scheme for water quality monitoring in a distribution network. *Int. J. Environ. Dev.* **2012**, *9*, 69–81.
15. Afshar, A.; Khombi, S.M. Multiobjective optimization of sensor placement in water distribution networks; dual use benefit approach. *Int. J. Optim. Civil. Eng.* **2015**, *5*, 315–331.
16. Cozzolino, L.; Mucherino, C.; Pianese, D.; Pirozzi, F. Positioning, within water distribution networks, of monitoring stations aiming at an early detection of intentional contamination. *Civ. Eng. Environ. Syst.* **2006**, *23*, 161–174. [[CrossRef](#)]
17. Ostfeld, A.; Uber, J.G.; Salomons, E.; Berry, J.W.; Hart, W.E.; Phillips, C.A.; Watson, J.P.; Dorini, G.; Jonkergouw, P.; Kapelan, Z.; et al. The battle of the water sensor networks (BWSN): A design challenge for engineers and algorithms. *J. Water Resour. Plan. Manag.* **2008**, *134*, 556–568. [[CrossRef](#)]
18. Laird, C.D.; Biegler, L.T.; van Bloemen Waanders, B.G.; Bartlett, R.A. Contamination source determination for water networks. *J. Water Resour. Plan. Manag.* **2005**, *131*, 125–134. [[CrossRef](#)]
19. Yan, X.; Gong, W.; Wu, Q. Contaminant source identification of water distribution networks using cultural algorithm. *Concurr. Comput. Pract. Exp.* **2017**, *29*, e4230. [[CrossRef](#)]
20. Zechman, E.M.; Ranjithan, S.R. Evolutionary computation-based methods for characterizing contaminant sources in a water distribution system. *J. Water Resour. Plan. Manag.* **2009**, *135*, 334–343. [[CrossRef](#)]
21. De Sanctis, A.; Boccelli, D.; Shang, F.; Uber, J. Probabilistic approach to characterize contamination sources with imperfect sensors. In Proceedings of the World Environmental and Water Resources Congress 2008, Ahupua'A, HI, USA, 13–16 May 2008; pp. 1–10.
22. Liu, L.; Ranjithan, S.R.; Mahinthakumar, G. Contamination source identification in water distribution systems using an adaptive dynamic optimization procedure. *J. Water Resour. Plan. Manag.* **2010**, *137*, 183–192. [[CrossRef](#)]
23. Liu, L.; Zechman, E.M.; Brill, E.D., Jr.; Mahinthakumar, G.; Ranjithan, S.; Uber, J. Adaptive contamination source identification in water distribution systems using an evolutionary algorithm-based dynamic optimization procedure. In Proceedings of the Eighth Annual Water Distribution Systems Analysis Symposium, Cincinnati, OH, USA, 27–30 August 2006; pp. 1–9.
24. Adedeji, K.B.; Hamam, Y.; Abe, B.T.; Abu-Mahfouz, A.M. Leakage Detection and Estimation Algorithm for Loss Reduction in Water Piping Networks. *Water* **2017**, *9*, 773. [[CrossRef](#)]
25. Hamam, Y.; Brameller, A. Hybrid method for the solution of piping networks. In *Proceedings of the Institution of Electrical Engineers*; IET: London, UK, 1971; Volume 118, pp. 1607–1612.
26. Hamam, Y.; Hindi, K. Optimised on-line leakage minimisation in water piping networks using neural nets. In Proceedings of the IFIP Working Conference, Dagschul, Germany, 28 September–1 October 1992; Volume 28, pp. 57–64.
27. Todini, E. A unifying view on the different looped pipe network analysis algorithms. In *Computing and Control for the Water Industry*; Research Studies Press Ltd.: Baldock, UK, 1999; pp. 63–80.
28. De Sanctis, A.E.; Shang, F.; Uber, J.G. Real-time identification of possible contamination sources using network backtracking methods. *J. Water Resour. Plan. Manag.* **2009**, *136*, 444–453. [[CrossRef](#)]
29. Wang, H.; Harrison, K.W. Improving efficiency of the Bayesian approach to water distribution contaminant source characterization with support vector regression. *J. Water Resour. Plan. Manag.* **2012**, *140*, 3–11. [[CrossRef](#)]

30. Huang, J.J.; McBean, E.A.; James, W. Multi-objective optimization for monitoring sensor placement in water distribution systems. In Proceedings of the Eighth Annual Water Distribution Systems Analysis Symposium Cincinnati, OH, USA, 27–30 August 2006; pp. 1–14.
31. Van Bloemen Waanders, B.G.; Bartlett, R.A.; Biegler, L.T.; Laird, C.D. Nonlinear programming strategies for source detection of municipal water networks. In Proceedings of the World Water & Environmental Resources Congress 2003, Philadelphia, PA, USA, 23–26 June 2003; pp. 1–10.
32. Laird, C.D.; Biegler, L.T.; van Bloemen Waanders, B.G. Real-time, large-scale optimization of water network systems using a subdomain approach. In *Real-Time PDE-Constrained Optimization*; SIAM: Philadelphia, PA, USA, 2007; pp. 289–306.
33. Preis, A.; Ostfeld, A. A contamination source identification model for water distribution system security. *Eng. Optim.* **2007**, *39*, 941–947. [[CrossRef](#)]
34. Rossman, L.A. *EPANET 2: Users Manual*; National Risk Management Research Laboratory, U.S. Environmental Protection Agency: Cincinnati, OH, USA, 2000.
35. Preis, A.; Ostfeld, A. Multiobjective sensor design for water distribution systems security. In Proceedings of the Eighth Annual Water Distribution Systems Analysis Symposium, Cincinnati, OH, USA, 27–30 August 2006; pp. 1–17.
36. Yan, X.; Zhao, J.; Hu, C.; Wu, Q. Contaminant source identification in water distribution network based on hybrid encoding. *J. Comput. Methods Sci. Eng.* **2016**, *16*, 379–390. [[CrossRef](#)]
37. Dawsey, W.J.; Minsker, B.S.; VanBlaricum, V.L. Bayesian belief networks to integrate monitoring evidence of water distribution system contamination. *J. Water Resour. Plan. Manag.* **2006**, *132*, 234–241. [[CrossRef](#)]
38. Tao, T.; Huang, H.D.; Xin, K.L.; Liu, S.M. Identification of contamination source in water distribution network based on consumer complaints. *J. Cent. South Univ. Technol.* **2012**, *19*, 1600–1609. [[CrossRef](#)]
39. Neupauer, R.M.; Records, M.K.; Ashwood, W.H. Backward probabilistic modeling to identify contaminant sources in water distribution systems. *J. Water Resour. Plan. Manag.* **2009**, *136*, 587–591. [[CrossRef](#)]
40. Wang, C.; Zhou, S. Contamination source identification based on sequential Bayesian approach for water distribution network with stochastic demands. *IIEE Trans.* **2017**, *49*, 899–910. [[CrossRef](#)]
41. Barandouzi, M.; Kerachian, R. Probabilistic Contaminant Source Identification in Water Distribution Infrastructure Systems. *Civ. Eng. Infrastruct. J.* **2016**, *49*, 311–326.
42. Di Nardo, A.; Di Natale, M.; Guida, M.; Musmarra, D. Water network protection from intentional contamination by sectorization. *Water Resour. Manag.* **2013**, *27*, 1837–1850. [[CrossRef](#)]
43. Kim, M.; Choi, C.Y.; Gerba, C.P. Source tracking of microbial intrusion in water systems using artificial neural networks. *Water Res.* **2008**, *42*, 1308–1314. [[CrossRef](#)] [[PubMed](#)]
44. Liu, L.; Zechman, E.M.; Mahinthakumar, G.; Ranji Ranjithan, S. Identifying contaminant sources for water distribution systems using a hybrid method. *Civ. Eng. Environ. Syst.* **2012**, *29*, 123–136. [[CrossRef](#)]
45. Liu, L.; Zechman, E.M.; Mahinthakumar, G.; Ranjithan, S.R. Coupling of logistic regression analysis and local search methods for characterization of water distribution system contaminant source. *Eng. Appl. Artif. Intell.* **2012**, *25*, 309–316. [[CrossRef](#)]
46. Brumbelow, K.; Torres, J.; Guikema, S.; Bristow, E.; Kanta, L. Virtual cities for water distribution and infrastructure system research. In Proceedings of the World Environmental and Water Resources Congress 2007: Restoring our Natural Habitat, Tampa, FL, USA, 15–19 May 2007; pp. 1–7.
47. Adedeji, K. Development of a Leakage Detection and Localisation Technique for Real-Time Applications in Water Distribution Networks. Ph.D. Thesis, Tshawane University of Technology, Pretoria, South Africa, 2018.
48. Basha, H.; Kassab, B. Analysis of water distribution systems using a perturbation method. *Appl. Math. Model.* **1996**, *20*, 290–297. [[CrossRef](#)]
49. Shockling, M.; Allen, J.; Smits, A. Roughness effects in turbulent pipe flow. *J. Fluid Mech.* **2006**, *564*, 267–285. [[CrossRef](#)]

50. Ozger, S.S.; Mays, L. A Semi-Pressure-Driven Approach to Reliability Assessment of Water Distribution Networks. Ph.D. Thesis, Arizona State University, Tempe, AZ, USA, 2003.
51. Kumar, S.M.; Narasimhan, S.; Bhallamudi, S.M. State estimation in water distribution networks using graph-theoretic reduction strategy. *J. Water Resour. Plan. Manag.* **2008**, *134*, 395–403. [[CrossRef](#)]



© 2019 by the authors. Licensee MDPI, Basel, Switzerland. This article is an open access article distributed under the terms and conditions of the Creative Commons Attribution (CC BY) license (<http://creativecommons.org/licenses/by/4.0/>).